High resolution spectroscopy of six SOCl2 isotopologues from the microwave to the far-infrared

M. A. Martin-Drumel, A. Roucou, G. G. Brown, S. Thorwirth, O. Pirali, G. Mouret, F. Hindle, M. C. McCarthy, and A. Cuisset

Citation: The Journal of Chemical Physics **144**, 084305 (2016); doi: 10.1063/1.4942024
View online: http://dx.doi.org/10.1063/1.4942024
View Table of Contents: http://scitation.aip.org/content/aip/journal/jcp/144/8?ver=pdfcov
Published by the AIP Publishing

High resolution spectroscopy of six $SOCl_2$ isotopologues from the microwave to the far-infrared

M. A. Martin-Drumel,[1,a)] A. Roucou,[2] G. G. Brown,[3] S. Thorwirth,[4] O. Pirali,[5] G. Mouret,[2] F. Hindle,[2] M. C. McCarthy,[1] and A. Cuisset[2]
[1]*Harvard-Smithsonian Center for Astrophysics, Cambridge, Massachusetts 02138, USA and School of Engineering and Applied Science, Harvard University, Cambridge, Massachusetts 02138, USA*
[2]*Laboratoire de Physico-Chimie de l'Atmosphère, Université du Littoral Côte d'Opale, Dunkerque, France*
[3]*Coker College, Hartsville, South Carolina 29550, USA*
[4]*I. Physikalisches Institut, Universität zu Köln, Köln, Germany*
[5]*AILES Beamline, Synchrotron SOLEIL, Saint Aubin, France*

(Received 26 October 2015; accepted 28 January 2016; published online 24 February 2016)

Despite its potential role as an atmospheric pollutant, thionyl chloride, $SOCl_2$, remains poorly characterized in the gas phase. In this study, the pure rotational and ro-vibrational spectra of six isotopologues of this molecule, all detected in natural abundance, have been extensively studied from the cm-wave band to the far-infrared region by means of three complementary techniques: chirped-pulse Fourier transform microwave spectroscopy, sub-millimeter-wave spectroscopy using frequency multiplier chain, and synchrotron-based far-infrared spectroscopy. Owing to the complex line pattern which results from two nuclei with non-zero spins, new, high-level quantum-chemical calculations of the hyperfine structure played a crucial role in the spectroscopic analysis. From the combined experimental and theoretical work, an accurate semi-experimental equilibrium structure (r_e^{SE}) of $SOCl_2$ has been derived. With the present data, spectroscopy-based methods can now be applied with confidence to detect and monitor this species, either by remote sensing or *in situ*. © *2016 AIP Publishing LLC.* [http://dx.doi.org/10.1063/1.4942024]

I. INTRODUCTION

Thionyl chloride, $SOCl_2$, is a versatile industrial compound with a global production measured in tens of thousands of tons per year. It is widely used as a chlorinating reagent in the industrial production of organochlorine compounds.[1–4] Thionyl chloride is also the cathode material in Li–$SOCl_2$ batteries which are characterized by remarkably high energy density and long lifetime.[5] However, safety concerns raised by the handling of the highly toxic content of these non-rechargeable cells have limited their use to industrial and commercial applications.[6] Improper disposal of $SOCl_2$ may have a significant pollution effect, particularly in the troposphere where the hydrolysis of this volatile molecule may release HCl and SO_2 within a few minutes.[2,3,7] Furthermore, the US threshold of toxicity (irreversible effects) for $SOCl_2$ is several ppm for an exposure of 10 min to 1 h.[8] While various types of toxic gas detectors are commercially available or have been described in the literature,[9] only a few have demonstrated $SOCl_2$ detection capability. In 2008, Lee and Strano[10] detected thionyl chloride at 0.7 ppb using a single walled carbon nanotube sensor functionalized with a polymer amine. However, the reproducibility of this detector is poor with detection limit varying significantly from one device to another (0.1–15 ppb). Furthermore, the molecule-specific selectivity has not been demonstrated, either with respect to competing substances such as chlorine and hydrochloric acid or even to water vapor of the atmosphere. More generally, some portable detection devices are able to identify many different chemical species using, for instance, ion mobility spectrometry or flame photometry.[11,12] Usually, these techniques are very sensitive but not selective; a pollutant can therefore easily be masked by another, unrelated compound. To address the issue of selectivity, next generation sensitive trace gas detectors will most likely exploit sensors in the sub-millimeter (submm) and terahertz (THz) domain, where observed transitions are molecule-specific.[13] In case of $SOCl_2$, however, rotational transitions in this frequency region remain unknown.

Motivated by the industrial and environmental importance of $SOCl_2$, numerous studies of its electrochemistry,[14] kinetics,[15] hydrolysis,[2,3] and photodissociation[16,17] have been performed. With respect to gas phase spectroscopic investigation, structural parameters have been derived from electron and X-ray diffraction studies,[18,19] the visible-ultraviolet spectrum has been recorded,[20] and the fundamental vibrational modes have been observed at low resolution by infrared (IR) and Raman spectroscopy.[21,22] High resolution measurements, however, have been extremely limited. Long restricted to pure rotational spectroscopy in the microwave (MW) spectral region,[23] they were recently extended (by some of us) to the far-infrared (FIR), where two low-lying vibrational modes (ν_3 and ν_6) were characterized.[4] $SOCl_2$ is a highly asymmetric top molecule ($\kappa = -0.448$ for the main isotopologue) belonging to the C_s point group owing to its plane of symmetry (Figure 1). Despite its relatively small size, its rotational and ro-vibrational spectra are extremely

a)Electronic mail: mmartin@cfa.harvard.edu

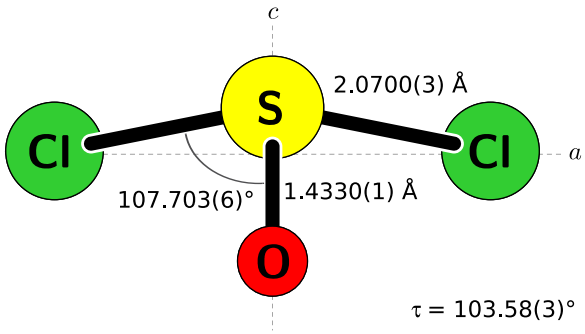

FIG. 1. Molecular structure of $SOCl_2$. Best-fit bond lengths and angles from the semi-experimental structure determined in this study (errors are quoted in parentheses). τ is the dihedral angle D(Cl.S.O.Cl).

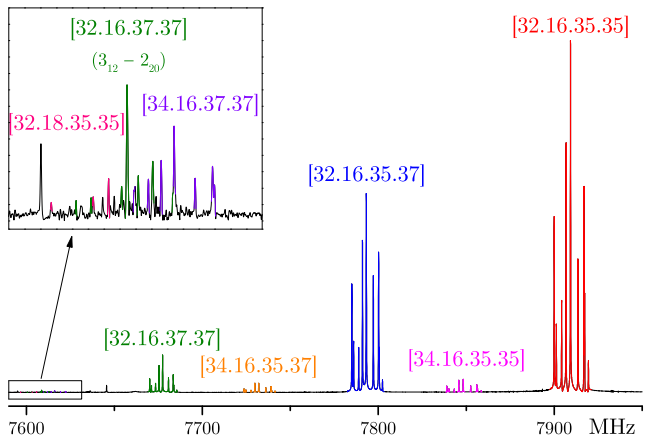

FIG. 2. Portion of the chirped-pulse spectrum showing the $1_{10}-0_{00}$ transition of different isotopologues of $SOCl_2$. The structure of each transition is dominated by the nuclear quadrupole hyperfine structure of the Cl nuclei.

dense because (i) $SOCl_2$ is a relatively heavy molecule and consequently possesses small rotational constants and (ii) the symmetry plane corresponds to the *bc* inertial plane and the two components of the dipole moment along these two principal axes of inertia are similar in magnitude, yielding *b*- and *c*-type transitions of comparable intensity in the pure rotation spectrum. That spectrum is further complicated by the presence of several abundant isotopologues (Table I) and two Cl atoms which produce resolvable nuclear quadrupole structure in the MW region (Figure 2).

The pure rotational spectrum of $SOCl_2$ has previously been measured in the MW band for the three most abundant isotopologues, $^{32}S^{16}O^{35}Cl^{35}Cl$, $^{32}S^{16}O^{35}Cl^{37}Cl$, and $^{32}S^{16}O^{37}Cl^{37}Cl$ (referred to hereafter as [32,16,35,35], [32,16,35,37], and [32,16,37,37] for the sake of simplicity) yielding accurate spectroscopic parameters for these species[23–33] and allowing the determination of the r_0 structure.[27,28] The determination of the nuclear quadrupole constants has proven more challenging since the S–Cl bond does not lie in any of the three planes defined by the principal axes of inertia, which results in non-zero off-diagonal coupling constants. Consequently, the six diagonal and off-diagonal constants have only been determined for the main isotopologue by means of Fourier-transform MW (FTMW) spectroscopy.[23]

TABLE I. Absolute and relative abundance of $SOCl_2$ isotopologues.

	Abundance (%)	
Species	*Absolute*	*Relative*
[32,16,35,35]	54.42	100.00[a]
[32,16,35,37]	34.80	63.96[a]
[32,16,37,37]	5.57	10.23[a]
[34,16,35,35]	2.41	4.43[a]
[34,16,35,37]	1.54	2.83[a]
[33,16,35,35]	0.43	0.79
[33,16,35,37]	0.27	0.50
[34,16,37,37]	0.25	0.45[a]
[32,18,35,35]	0.11	0.21
[32,18,35,37]	0.07	0.13
[33,16,37,37]	0.04	0.08
[32,18,37,37]	0.01	0.02

[a]Species studied in this work.

In the present study, high resolution investigations of the pure rotational and ro-vibrational spectra of six isotopologues of $SOCl_2$ — [32.16.35.35], [32.16.35.37], [32.16.37.37], [34.16.35.35], [34.16.35.37], and [34.16.37.37], all detected in natural abundance — have been undertaken from the MW to the FIR, using three complementary experimental approaches: (i) chirped-pulse FTMW (CP-FTMW) spectroscopy; (ii) submm spectroscopy using a frequency multiplication chain; and (iii) synchrotron-based FT-FIR spectroscopy. The 7 to 19 GHz CP-FTMW spectrum of $SOCl_2$ reveals pure rotational transitions of all six isotopologues studied here, with resolved chlorine nuclear quadrupole structure. Additional pure rotational transitions in the ground vibrational state of [32.16.35.35], [32.16.35.37], and [32.16.37.37] have been recorded in the 70–660 GHz region. Finally, the rovibrational spectra of the symmetric ν_3 (344 cm^{-1}) and asymmetric ν_6 (284 cm^{-1}) fundamental bands of [32.16.35.37] and [32.16.37.37] have been resolved. Accurate spectroscopic parameters of each species (rotational, centrifugal distortion (CD), and nuclear quadrupole constants; vibrational band centers) have been determined from fits of all these data. From these highly accurate experimental rotational constants and quantum-chemical calculations, a highly accurate semi-experimental (SE) equilibrium structure (r_e^{SE}) has been derived for the molecule.

II. EXPERIMENTS AND THEORETICAL CALCULATIONS

A. Chirped-pulse FTMW spectroscopy

The broadband spectrum of $SOCl_2$ has been measured in the 7–19 GHz region using CP-FTMW spectroscopy.[34] A gaseous mixture of 0.5% of the molecule heavily diluted in neon, at a backing pressure of 3.3 bars, was supersonically expanded into the vacuum chamber via a pulsed nozzle operating at 5 Hz. Details on the design on the pulsed nozzle can be found in Ref. 35. The chirps from our arbitrary waveform generator (AWG) are 4 μs in duration, span 0.5–11.5 GHz, and are repeated every 20 μs. Because the gas pulse is long (~1 ms)

compared to the dephasing time (~10 μs) of the free induction decay (FID), 10 chirps can be used to interrogate each gas pulse. The total recorded FID consists of 750,000 points, each separated by 2 ps. The first 5 μs of this FID contains the chirp, and the remaining 10 μs are Fourier-transformed, resulting in a resolution of 100 kHz in the frequency domain.

A total of 4×10^6 FIDs was recorded and averaged in about 20 h. The resulting rotational spectrum, obtained by Fourier transforming the FID, presents a very high signal-to-noise ratio (SNR), as evidenced in Figure 2. The time domain spectrum was post-zero-filled by a factor of 16 prior to Fourier transformation, yielding points spaced by about 7 kHz in the frequency domain. The central frequency of each transition has been determined from a search of local maxima in the spectrum; no attempt has been made to fit individual line profiles. Owing to the wide range of SNR, uncertainties have been derived for each transition using the empirical equation

$$\Delta\nu = \Delta_{\text{shape}} + \Delta_{\text{spacing}} = \frac{\text{FWHM}}{2\text{SNR}} + \frac{\delta}{2}, \quad (1)$$

where FWHM is the full-width half-maximum of the line, typically 300 kHz in this study, and δ the frequency step. The first term of the equation is a well-known expression used in conventional FT infrared spectroscopy,[36] while the second one arises from our peak finding algorithm, i.e., $\delta = 7$ kHz in this study. Using this equation, $\Delta\nu$ as low as 10 kHz have been calculated for some transitions. To simplify the uncertainties, the values obtained from Equation (1) have been rounded to steps of 5 kHz. The validity of Equation (1) was first verified on [32.16.35.35] by comparing the very accurate frequencies from Müller and Gerry[23] (to better than 1 kHz) to our experimental frequencies and their associated errors calculated using Equation (1). Additional details of this procedure are presented in supplementary material S1.[37]

In addition to the main isotopologue, transitions of five isotopic species — [32.16.35.37], [32.16.37.37], [34.16.35.35], [34.16.35.37], and [34.16.37.37] — were observed and assigned. Transitions of the ^{33}S isotopic species have also been identified, but no attempt was made to assign them considering that the presence of a third nuclear quadrupole yields an even more complex hyperfine pattern. Finally, some transitions of [32.18.35.35] have been observed but these lines are quite weak and spectral congestion prevented any definite assignment (Fig. 2).

B. Sub-millimeter spectroscopy

The absorption spectrum of $SOCl_2$ has been recorded at room temperature in the submm domain. A continuous flow of 15 μbar of the sample, maintained by a roughing pumping, was passed through a 120 cm-long and 56 mm-diameter single-path absorption cell and probed by the radiation generated from a frequency multiplier chain (Virginia Diodes, Inc). Two off-axis parabolic mirrors are used to collimate the radiation into the cell and then refocused it onto a liquid helium cooled InSb bolometer.[38–40] The spectrum has been recorded in the 70–110 and 140–660 GHz regions using a frequency modulation of 60 kHz, 11 kHz modulation depth of the frequencies delivered by the synthesizer, a time constant of 10 ms, and 100 kHz frequency steps. Pure rotational transitions of the three most abundant isotopologues of $SOCl_2$— [32.16.35.35], [32.16.35.37], and [32.16.37.37] — in their ground vibrational state have been assigned in the spectrum (Figure 3).

C. Fourier-transform far-infrared spectroscopy

In a recent study by several of us,[4] the high resolution (0.001 cm^{-1}) FT-FIR spectrum of $SOCl_2$ was recorded at the SOLEIL synchrotron facility and the ν_3 and ν_6 ro-vibrational bands of [32.16.35.35] were analyzed. We report here further study of this spectrum which has enabled the assignment of transitions in these two bands for [32.16.35.37] and [32.16.37.37], both detected in natural abundance (Figure 4). All experimental details (beamsplitter, detector, absorption length, etc.) have been reported previously.[4]

III. QUANTUM-CHEMICAL CALCULATIONS

The high-resolution spectroscopic study of $SOCl_2$ presented here was complemented with quantum-chemical calculations performed at the coupled-cluster singles and doubles (CCSD) level augmented by a perturbative treatment of triple excitations, CCSD(T).[41] All calculations were performed using the program suite CFOUR[42] in combination with basis sets from Dunning's hierarchies of correlation consistent polarized valence and polarized core-valence sets [cc-pVXZ, cc-pV(X + d)Z, and cc-pwCVXZ with X = T and Q].[43] Equilibrium molecular structures were calculated using analytic gradient techniques.[44] The theoretical best-estimate structure was calculated at the CCSD(T)/cc-pwCVQZ level of theory (considering all electrons in the correlation treatment) which has been shown earlier to provide equilibrium structural parameters of very high quality.[45–47] The chlorine equilibrium nuclear quadrupole coupling and spin-rotation constants were derived at the same level of theory (the latter employing perturbation-dependent basis functions[48]) to support the analysis of the complex hyperfine structure observed in the pure rotational spectra of $SOCl_2$. Harmonic and anharmonic

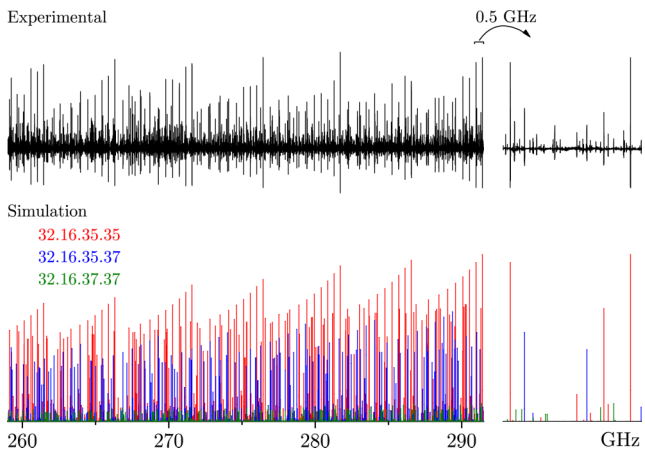

FIG. 3. Portion of the sub-millimeter spectrum of $SOCl_2$ (upper traces) and comparison with simulation (stick spectrum) of the pure rotational spectrum of [32.16.35.35], [32.16.35.37], and [32.16.37.37] (lower traces). Transitions in the experimental spectrum show a typical second derivative shape.

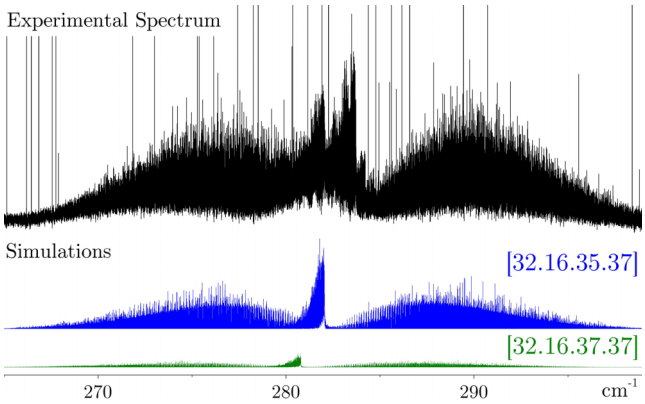

FIG. 4. Experimental FT-FIR spectrum of the ν_6 band of $SOCl_2$ compared with simulated spectra for the [32.16.35.37] and [32.16.37.37] isotopologues. The strongest Q-branch feature on the experimental spectrum, which is not reproduced by the simulations, arises from [32.16.35.35] (its analysis has been published previously[4]). The contribution of [32.16.35.37] to slightly lower energy is clearly visible, as well as hot-band Q-branches to high wavenumber from the one for the fundamental of [32.16.35.35]. Strong individual lines in the experimental spectrum arise from residual water in the absorption cell.

force fields were calculated in the frozen-core approximation at the CCSD(T)/cc-pV(T+*d*)Z level of theory using analytic second-derivative techniques[49,50] followed by additional numerical differentiation to calculate the third and fourth derivatives needed for the anharmonic force fields.[50,51] The calculated zero-point vibrational corrections (ΔA_0, ΔB_0, and ΔC_0) and the experimental ground state rotational constants were then used to determine semi-experimental equilibrium rotational constants from the relation $B_e^{SE} = B_0 + \Delta B_0$ (with similar relations for A_e^{SE} and C_e^{SE}, respectively) which themselves were directly converted into semi-experimental moments of inertia for the molecular structure determination. A review of the methods and strategies employed here has been given recently elsewhere.[52] See supplementary material S2 for detailed results of the quantum-chemical calculations.[37]

IV. RESULTS AND DISCUSSION

For [32.16.35.35], [32.16.35.37], and [32.16.37.37], pure rotational transitions have been assigned up to 660 GHz on the MW and submm spectra. Additionally, for [32.16.35.37] and [32.16.37.37], ro-vibration transitions in the ν_3 and ν_6 bands have been assigned in the FT-FIR spectrum. Finally, pure rotational transitions of [34.16.35.35], [34.16.35.37], and [34.16.37.37] have been assigned up to about 18 GHz in the MW spectrum. Complete lists of assigned transitions are provided in supplementary material S3.[37]

A. Determination of the molecular constants

Effective fits have been performed for each isotopologue using the SPFIT/SPCAT suite of programs[53] in which the present new measurements and all available transitions from the literature, i.e., from Refs. 4, 23, 24, and 29 for [32.16.35.35] and Refs. 29, 31, and 32 for [32.16.35.37], have been included. MW transitions have been weighted according to Equation (1), while for the submm and FIR transitions, a single uncertainty — 100 kHz and 0.0003 cm^{-1}, respectively — has been used in the fits. Individual unitless standard deviations are close to unity for all fits, as illustrated by Table II, a likely indication of the robustness of the fit. The complete list of molecular parameters for all isotopologues, including nuclear quadrupole coupling constants and rotational constants in vibrationally excited states, is presented in supplementary material S4.[37]

Table III presents the extensive list of ground state rotational and centrifugal distortion (CD) constants, as well as the ν_3 and ν_6 band centers, derived for [32.16.35.35], [32.16.35.37], and [32.16.37.37] (nuclear quadrupole coupling parameters are omitted from this table but can be found in supplementary material S4[37]). In particular, all quartic and sextic CD terms, as well as one octic term (L_K), are determined for these three species. The use of three broadband rotationally resolved techniques has enabled the determination of an extensive list of precise spectroscopic parameters and allows the most intense rotational transitions of $SOCl_2$ to be predicted to very high accuracy from the MW to the FIR. For trace gas detection, accurate frequency lists in the terahertz domain should be particularly valuable for [32.16.35.35].

It is also worth emphasizing that reproducing the nuclear quadrupole structure which is well resolved in the MW

TABLE II. Summary of the number of fitted frequencies (N)[a] highest quantum numbers and standard deviation for the six fits performed in this study.

	Transitions				Standard deviation		
	N	N[b]	J''_{max}	$K''_{a\,max}$	MW[c]/MHz	IR[d]/cm^{-1}	Unitless
[32.16.35.35]	18 209	8 706	127	71	0.095	0.000 12	1.05
[32,16,35,37]	15 341	15 260	117	65	0.090	0.000 30	1.07
[32,16,37,37]	8 274	8 274	100	64	0.100	0.000 33	1.07
[34,16,35,35]	137	137	4	2	0.060		0.85
[34,16,35,37]	67	67	2	1	0.073		1.25
[34,16,37,37]	23	23	1	1	0.054		1.10

[a] N represents the number of different frequencies in the fit, including resolved nuclear quadrupole structure. For instance, in case of [34,16,37,37], 3 rotational transitions were observed, each of which was split into several hyperfine components yielding 23 frequencies assigned. At high frequency, many asymmetric splittings are unresolved in the submm and FIR spectra, and thus appear as a single frequency in this summary.
[b] This work.
[c] MW and submm data.
[d] FIR data.

TABLE III. Ground state rotational and centrifugal distortion constants, and ν_3 and ν_6 band centers of the three most abundant isotopologues of $SOCl_2$ (in MHz, unless overwise noted; 1σ uncertainties are quoted in parentheses in the unit of the last digit).

	[32.16.35.35]	[32.16.35.37]	[32.16.37.37]
A	5086.748 241 (12)	5044.367 26 (12)	4999.220 44 (35)
B	2822.530 074 (11)	2748.942 284 (58)	2678.227 08 (19)
C	1960.313 909 5 (89)	1918.657 939 (64)	1877.820 32 (21)
$\Delta_J \times 10^3$	1.125 143 3 (38)	1.072 539 0 (99)	1.024 996 (48)
$\Delta_{JK} \times 10^3$	−2.226 670 (30)	−2.133 200 (42)	−2.069 98 (22)
$\Delta_K \times 10^3$	6.986 77 (10)	6.868 75 (12)	6.780 97 (56)
$\delta_J \times 10^3$	0.394 367 4 (17)	0.373 417 9 (45)	0.354 872 (23)
$\delta_K \times 10^3$	1.248 389 (35)	1.230 531 (46)	1.203 33 (23)
$\Phi_J \times 10^9$	0.417 63 (32)	0.381 96 (60)	0.363 8 (46)
$\Phi_{JK} \times 10^9$	5.671 1 (65)	5.412 0 (74)	5.142 (60)
$\Phi_{KJ} \times 10^6$	−0.041 569 (20)	−0.039 786 (22)	−0.038 40 (18)
$\Phi_K \times 10^6$	0.059 289 (49)	0.058 111 (52)	0.057 01 (37)
$\phi_J \times 10^9$	0.222 06 (15)	0.203 43 (31)	0.198 4 (24)
$\phi_{JK} \times 10^9$	1.203 0 (42)	1.168 2 (54)	0.942 (40)
$\phi_K \times 10^6$	0.017 014 (21)	0.016 739 (23)	0.016 10 (21)
$L_K \times 10^{12}$	−0.121 4 (71)	−0.226 4 (62)	−0.335 (71)
ν_6 (in cm^{-1})	283.725 599 6 (63)	282.058 493 (13)	280.805 593 (14)
ν_3 (in cm^{-1})	345.966 589 3 (57)	344.111 151 (11)	342.405 878 (16)

spectrum for the six species studied here is non-trivial, since both diagonal and off-diagonal parameters are required to correctly describe this particular molecule and only a few rotational transitions are accessible in this spectral region. In this regard, high-level calculations concurrently with the experimental studies have been invaluable in the spectroscopic analysis. The calculated nuclear quadrupole coupling constants are found to be extremely accurate allowing one to reproduce the hyperfine pattern of individual lines in the spectrum to measurement uncertainty by varying only a small subset of the possible hyperfine parameters (see supplementary material S4[37]).

B. Geometry determination

Table IV presents the experimental ground state and semi-experimental equilibrium rotational constants of all six isotopologues studied in this work. From these values, it has been possible to derive a semi-experimental equilibrium structure (r_e^{SE}) using the STRFIT software developed by Kisiel.[54] Apart from [34.16.37.37], for which C_0 could not be determined (only three rotational transitions were observed, two of which of the same type), all three rotational constants of each species have been used in the structural determination. The derived values are presented in Figure 1 and Table V. In Table V, the SE parameters are compared to purely theoretical ones calculated at the CCSD(T)/cc-pwCVQZ level of theory; the agreement is excellent. These parameters are also very close to those determined experimentally from electron diffraction measurements.[19] The sulfur-oxygen bond length r(S–O) in $SOCl_2$ is comparable to the one found in SO_2, 1.433(1) Å vs. 1.431 Å,[45,55] and hence in the typical S-O double bond regime. The sulfur-chlorine distance r(S–Cl) = 2.070(1) Å is substantially longer compared to the one of 2.014 Å determined in sulfur dichloride, SCl_2,[45,56] being indicative of pronounced single-bond character.

Although the present structural analysis lacks the observation of oxygen isotopic species, inclusion of the ^{18}O data will most likely only change the present values by a fraction of the current error. At present, many more rotational constants (17, 12 of which are uncorrelated) relative

TABLE IV. Experimental ground state and semi-experimental equilibrium rotational constants of the six isotopologues of $SOCl_2$ studied in this work (see supplementary material S4 for complete values, including errors[37]). For [34.16.37.37], C_0 could not be determined (only three rotational transitions observed, two of which are of the same type) and was thus not used for the structure determination.

	[32.16.35.35]	[32.16.35.37]	[32.16.37.37]	[34.16.35.35]	[34.16.35.37]	[34.16.37.37]
A_0	5086.748	5044.367	4999.220	5031.663	4988.866	4943.194
B_0	2822.530	2748.942	2678.227	2816.642	2743.283	2672.902
C_0	1960.314	1918.658	1877.820	1955.002	1913.350	
A_e	5099.056	5056.584	5011.326	5043.571	5000.693	4954.898
B_e	2833.354	2759.397	2688.336	2827.317	2753.583	2682.874
C_e	1969.730	1927.807	1886.710	1964.304	1922.387	

TABLE V. Ground state (r_0) and equilibrium (r_e) structural parameters of $SOCl_2$ and comparison with values obtained by electron diffraction.[19]

	r_0		r_e		Electron
	Expt.[a]	Ref. 28	SE[b]	Calc.[c]	diffraction[19]
r(S–O) /Å	1.434 (9)	1.435 (4)	1.4330 (7)	1.432	1.4394 (10)
r(S–Cl) /Å	2.072 (3)	2.071 (2)	2.0700 (3)	2.071	2.0697[d]
α(Cl–S–O) /°	108.00 (6)	108.01 (17)	107.703 (6)	107.75	107.42[d]
α(Cl–S–Cl) /°	97.08[e]	97.167 (11)	96.929[e]	96.903[e]	96.30 (2)
τ(Cl.S.O.Cl) /°	104.0 (3)		103.58 (3)	103.59	

[a]Experimental, this work. Errors (3σ) are reported in the unit of the last digit.
[b]Semi-experimental, this work. Errors (3σ) are reported in the unit of the last digit.
[c]Calculated at the CCSD(T)/cc-pwCVQZ level of theory, this work.
[d]Mean values; r(S–Cl1) = 2.0745 (4) Å, r(S–Cl2) = 2.0648(4) Å, α(Cl1–S–O) = 107.30°, α(Cl2–S–O) = 107.54°.
[e]Derived values.

to the number of geometrical parameters (4) have been used. For this reason, the overall fit is well-constrained and the derived structural values can be considered highly reliable.

V. CONCLUSIONS AND PROSPECTS

In this study, the pure rotational and ro-vibrational spectra of $SOCl_2$ have been studied from the MW to the FIR using three complementary spectroscopic instruments (chirped-pulse FTMW spectrometer, frequency multiplier chain, and synchrotron-based FT-FIR spectrometer). Six isotopic species, including rare ones, have been detected in natural abundance. High-level quantum-chemical calculations were an invaluable tool in the analysis of the experimental data, particularly with respect to the nuclear quadrupole complex pattern resolved in the MW region. The accurate spectroscopic parameters determined for the six isotopologues studied, combined with high level quantum-chemical calculations, have enabled the first determination of a highly accurate semi-experimental equilibrium geometry (r_e^{SE}) of $SOCl_2$. Even though a tremendous number of transitions has been assigned in this work, many more lines (probably arising from vibrationally excited states) remain to be analyzed, particularly in the submm spectrum.

From the precise spectroscopic parameters determined in this study, an accurate list of frequencies can be predicted from the MW to the FIR for the strongest transitions of $SOCl_2$ which should be useful for future trace gas detection in the submm/THz domain. Now that rotational frequencies have been accurately determined, real-time monitoring of this toxic compound and its hydrolysis products may be undertaken under atmospheric conditions (pressure, temperature). Recently, several of us have demonstrated that the products from formaldehyde photolysis can be continuously monitored using a submm-wave spectrometer.[57] This kind of approach might be adapted to the $SOCl_2$ hydrolysis monitoring and might greatly benefit from the use of a chirped-pulse instrument in the submm-wave domain[13] which would enable rapid monitoring of both the reactant and its products, a critical consideration in chemical reactivity.

ACKNOWLEDGMENTS

The authors are grateful to SOLEIL for providing beamtime on the AILES beamline under Proposal No. 20100693. We thank Dr. P. Roy and her team (SOLEIL) and Dr. M. Guinet and Dr. S. Eliet (LPCA) for their help during the experiments at SOLEIL. The submm work is supported by the French "Délégation Générale pour l'Armement" (*Projet de Recherche Exploratoire et Innovation* No. 06.34.037) and the CP-FTMW experimental work is supported by NASA Grant No. NNX13AE59G. M.A.M.-D. is partially supported by a CfA Postdoctoral Fellowship from the Smithsonian Astrophysical Observatory. G.G.B. acknowledges the support of NSF Award No. 1213560. S.T. gratefully acknowledges support by the Deutsche Forschungsgemeinschaft (DFG) through Grant No. TH 1301/3-2. The authors are thankful to Dr. M. Goubet for providing the Ph.D. thesis of J. L. Journel.[29]

[1]H.-D. Lauss and W. Steffens, "Sulfur halides," in *Ullmann's Encyclopedia of Industrial Chemistry* (Wiley-VCH Verlag GmbH & Co. KGaA, 2000).
[2]T. J. Johnson, R. S. Disselkamp, Y. F. Su, R. J. Fellows, M. L. Alexander, and C. J. Driver, J. Phys. Chem. A **107**, 6183 (2003).
[3]S. K. Ignatov, P. G. Sennikov, A. G. Razuvaev, and O. Schrems, J. Phys. Chem. A **108**, 3642 (2004).
[4]M.-A. Martin-Drumel, G. Mouret, O. Pirali, and A. Cuisset, J. Mol. Spectrosc. **315**, 30 (2015).
[5]P. A. Mosier-Boss and S. Szpak, "Assessment of Li/$SOCl_2$ battery technology: Reserve, thin-cell design, volume 3," Technical Report No. 1154 (1990).
[6]S. C. Levy and P. Bro, *Battery Hazards and Accident Prevention* (Springer US, 1994), pp. 211–232.
[7]C. S. Yeung, P. L. Ng, X. G. Guan, and D. L. Phillips, J. Phys. Chem. A **114**, 4123 (2010).
[8]See http://www.epa.gov/sites/production/files/2014-09/documents/thionylchloride_tsd_interim_version_105_2008.pdf for "Acute exposure guideline levels (AEGL) for thionyl chloride."
[9]S.-H. Lim, J. Sens. Sci. Technol. **24**, 311 (2015).
[10]C. Y. Lee and M. S. Strano, J. Am. Chem. Soc. **130**, 1766 (2008).
[11]M. Utriainen, E. Kärpänoja, and H. Paakkanen, in *Proceedings of the Ninth International Meeting on Chemical Sensors* [Sens. Actuators, B **93**, 17 (2003)].
[12]Z.-J. Ding, P.-H. Wang, Z.-J. Li, B. Du, L. Guo, and J.-H. Yu, Spectrosc. Spectral Anal. **35**, 2025 (2015).
[13]E. Gerecht, K. O. Douglass, and D. F. Plusquellic, Opt. Express **19**, 8973 (2011).
[14]H. V. Venkatasetty, J. Electrochem. Soc. **127**, 2531 (1980).
[15]T. C. DeVore and T. N. Gallaher, Inorg. Chem. **23**, 3506 (1984).
[16]H. Wang, X. Chen, and B. R. Weiner, J. Phys. Chem. **97**, 12260 (1993).
[17]M. Roth, C. Maul, and K.-H. Gericke, Phys. Chem. Chem. Phys. **4**, 2932 (2002).

[18]I. Hargittai, Acta Chim. Acad. Sci. Hung. **60**, 231 (1969).
[19]D. Mootz and A. Merschenz-Quack, Acta Crystallogr., Sect. C: Cryst. Struct. Commun. **44**, 926 (1988).
[20]A. P. Uthman, P. J. Demlein, T. D. Allston, M. C. Withiam, M. J. McClements, and G. A. Takacs, J. Phys. Chem. **82**, 2252 (1978).
[21]R. Vogel-Hogler, Acta Phys. Austriaca **1**, 323 (1948).
[22]D. E. Martz and R. T. Lagemann, J. Chem. Phys. **22**, 1193 (1954).
[23]H. S. P. Müller and M. C. L. Gerry, J. Chem. Soc., Faraday Trans. **90**, 3473 (1994).
[24]J. Burie, J. L. Destombes, A. Dubrulle, and G. Journel, C. R. Hebd Seances Acad. Sci., Sér. B **267**, 48 (1968).
[25]G. Journel, A. Dubrulle, J. L. Destombe, and C. Marliere, C. R. Hebd Seances Acad. Sci., Sér. B **271**, 331 (1970).
[26]H. U. Wenger, A. Bauder, and H. H. Gunthard, Chem. Phys. **1**, 441 (1973).
[27]S. Suzuki, M. Yamaguchi, M. Onda, T. Sakaizumi, O. Ohashi, and I. Yamaguchi, J. Mol. Struct. **73**, 41 (1981).
[28]F. Mata and N. Carballo, J. Mol. Struct. **101**, 233 (1983).
[29]G. Journel, Ph.D. thesis, University of Lille, France, 1969.
[30]J. L. Destombes, Ph.D. thesis, University of Lille, France, 1970.
[31]A. Dubrulle and D. Boucher, C. R. Hebd Seances Acad. Sci. Sér. B **274**, 1426 (1972).
[32]I. Merke and H. Dreizler, Z. Naturforsch. A **47**, 1141 (1992).
[33]A. Dubrulle, Ph.D. thesis, University of Lille, France, 1972.
[34]G. G. Brown, B. C. Dian, K. O. Douglass, S. M. Geyer, S. T. Shipman, and B. H. Pate, Rev. Sci. Instrum. **79**, 053103 (2008).
[35]W. Chen, S. E. Novick, M. C. McCarthy, C. A. Gottlieb, and P. Thaddeus, J. Chem. Phys. **103**, 7828 (1995).
[36]S. P. Davis, M. C. Abrams, and J. W. Brault, *Fourier Transform Spectrometry* (Academic Press, 2001).
[37]See supplementary material at http://dx.doi.org/10.1063/1.4942024 for the determination of the accuracy on line frequency using CP-FTMW spectroscopy, the results of quantum-chemical calculations, the spectroscopic parameters, and all experimental frequencies and fit files.
[38]G. Mouret, M. Guinet, A. Cuisset, L. Croize, S. Eliet, R. Bocquet, and F. Hindle, IEEE Sens. J. **13**, 133 (2013).
[39]A. Cuisset, M.-A. Martin Drumel, F. Hindle, G. Mouret, and D. A. Sadovskii, Chem. Phys. Lett. **586**, 10 (2013).
[40]O. Pirali, Z. Kisiel, M. Goubet, S. Gruet, M. A. Martin-Drumel, A. Cuisset, F. Hindle, and G. Mouret, J. Chem. Phys. **142**, 104310 (2015).
[41]K. Raghavachari, G. W. Trucks, J. A. Pople, and M. Head-Gordon, Chem. Phys. Lett. **157**, 479 (1989).
[42]CFOUR, a quantum chemical program package written by J. F. Stanton, J. Gauss, M. E. Harding, and P. G. Szalay, with contributions from A. A. Auer, R. J. Bartlett, U. Benedikt, C. Berger, D. E. Bernholdt, Y. J. Bomble, L. Cheng, O. Christiansen, M. Heckert, O. Heun, C. Huber, T.-C. Jagau, D. Jonsson, J. Jusélius, K. Klein, W. J. Lauderdale, D. A. Matthews, T. Metzroth, L. A. Mück, D. P. O'Neill, D. R. Price, E. Prochnow, C. Puzzarini, K. Ruud, F. Schiffmann, W. Schwalbach, S. Stopkowicz, A. Tajti, J. Vázquez, F. Wang, and J. D. Watts and the integral packages MOLECULE (J. Almlöf and P. R. Taylor), PROPS (P. R. Taylor), ABACUS (T. Helgaker, H. J. Aa. Jensen, P. Jørgensen, and J. Olsen), and ECP routines by A. V. Mitin and C. van Wüllen. For the current version, see http://www.cfour.de; M. E. Harding, T. Metzroth, J. Gauss, and A. A. Auer, J. Chem. Theory Comput. **4**, 64 (2008).
[43]T. H. Dunning, J. Chem. Phys. **90**, 1007 (1989); T. H. Dunning, K. A. Peterson, and A. K. Wilson, *ibid.* **114**, 9244 (2001); D. E. Woon and T. H. Dunning, *ibid.* **103**, 4572 (1995).
[44]J. D. Watts, J. Gauss, and R. J. Bartlett, Chem. Phys. Lett. **200**, 1 (1992).
[45]S. Coriani, D. Marcheson, J. Gauss, C. Hättig, T. Helgaker, and P. Jørgensen, J. Chem. Phys. **123**, 184107 (2005).
[46]D. T. Halfen, D. J. Clouthier, L. M. Ziurys, V. Lattanzi, M. C. McCarthy, P. Thaddeus, and S. Thorwirth, J. Chem. Phys. **134**, 134302 (2011).
[47]S. Thorwirth, R. I. Kaiser, K. N. Crabtree, and M. C. McCarthy, Chem. Commun. **51**, 11305 (2015).
[48]J. Gauss, K. Ruud, and T. Helgaker, J. Chem. Phys. **105**, 2804 (1996).
[49]J. Gauss and J. F. Stanton, Chem. Phys. Lett. **276**, 70 (1997).
[50]J. F. Stanton and J. Gauss, Int. Rev. Phys. Chem. **19**, 61 (2000).
[51]J. F. Stanton, C. L. Lopreore, and J. Gauss, J. Chem. Phys. **108**, 7190 (1998).
[52]C. Puzzarini, J. F. Stanton, and J. Gauss, Int. Rev. Phys. Chem. **29**, 273 (2010).
[53]H. M. Pickett, J. Mol. Spectrosc. **148**, 371 (1991).
[54]Z. Kisiel, J. Mol. Spectrosc. **218**, 58 (2003).
[55]Y. Morino, M. Tanimoto, and S. Saito, Acta Chem. Scand., Ser. A **42**, 346 (1988).
[56]L. Bizzocchi, L. Cludi, C. Degli Esposti, and A. Giorgi, J. Mol. Spectrosc. **204**, 275 (2000).
[57]A. Omar, S. Eliet, A. Cuisset, G. Dhont, C. Coeur-Tourneur, R. Bocquet, G. Mouret, and F. Hindle, IEEE Sens. J. **15**, 6141 (2015).